Grapevines under drought do not express esca leaf symptoms

Giovanni Bortolami[a], Gregory A. Gambetta[b], Cédric Cassan[c,d], Silvina Dayer[b], Elena Farolfi[a], Nathalie Ferrer[a], Yves Gibon[c,d], Jérôme Jolivet[a], Pascal Lecomte[a], and Chloé E. L. Delmas [a,1]

[a]Institut National de Recherche pour l'Agriculture, l'Alimentation et l'Environnement (INRAE), Bordeaux Sciences Agro (BSA), Institut des Sciences de la Vigne et du Vin (ISVV), Santé et Agroécologie du Vignoble (SAVE), Villenave d'Ornon 33140, France; [b]Ecophysiologie et Génomique Fonctionnelle de la Vigne (EGFV), BSA, INRAE, Université de Bordeaux, ISVV, Villenave d'Ornon 33140, France; [c]Université Bordeaux, INRAE, UMR 1332 Biologie du Fruit et Pathologie, Centre INRAE Nouvelle-Aquitaine Bordeaux, Villenave d'Ornon 33140, France; and [d]Bordeaux Metabolome Facility, INRAE, Université Bordeaux, Centre INRAE Nouvelle-Aquitaine Bordeaux, Villenave d'Ornon 33140, France

Edited by Louis S. Santiago, University of California, Riverside, CA, and accepted by Editorial Board Member Sean R. Cutler September 1, 2021 (received for review July 13, 2021)

In the context of climate change, plant mortality is increasing worldwide in both natural and agroecosystems. However, our understanding of the underlying causes is limited by the complex interactions between abiotic and biotic factors and the technical challenges that limit investigations of these interactions. Here, we studied the interaction between two main drivers of mortality, drought and vascular disease (esca), in one of the world's most economically valuable fruit crops, grapevine. We found that drought totally inhibited esca leaf symptom expression. We disentangled the plant physiological response to the two stresses by quantifying whole-plant water relations (i.e., water potential and stomatal conductance) and carbon balance (i.e., CO_2 assimilation, chlorophyll, and nonstructural carbohydrates). Our results highlight the distinct physiology behind these two stress responses, indicating that esca (and subsequent stomatal conductance decline) does not result from decreases in water potential and generates different gas exchange and nonstructural carbohydrate seasonal dynamics compared to drought.

abiotic–biotic interactions | carbon balance | drought | plant dieback | vascular disease

For many plant pathogens, it is still largely unknown if their interactions with abiotic stresses are synergistic, antagonistic, or neutral. These interactions are particularly crucial in the case of vascular diseases and drought (1–3). Both affect the same plant tissue, the xylem vascular network, which is responsible for the movement of water and nutrients throughout the plant. A strong synergy when combining drought and vascular disease could accelerate plant death (1, 3) and has strong implications in the context of climate change, in which a global increase of drought and associated plant mortality is expected (4).

Grapevine, one of the most economically valuable crops in the world (5), is being threatened by future climate change scenarios (6). Since the early 2000s, old-world vineyards have exhibited increasing yield losses, and although the causes are not completely understood, an increased incidence of trunk diseases has been identified as one of the main contributors (7, 8). One of the most prominent of these diseases is esca. Esca is a vascular disease associated with losses in fruit quality and quantity and increased vine mortality, and the mechanisms of esca pathogenesis are still largely misunderstood (9, 10). This latent disease primarily affects perennial organs (i.e., the trunk), causing necrosis of internal tissues. Annual organs (i.e., leaves and clusters) typically begin to display symptoms in mature plants (normally older than 10 y) (11, 12). Recent work by our laboratory quantified the presence of hydraulic failure in the xylem tissue of esca-symptomatic leaves and stems (13, 14), and it is hypothesized that the transpiration stream facilitates the transport of phytotoxic metabolites from the pathogen niche in the trunk to the leaves (8). Therefore, the physiology controlling vine water use likely plays a crucial role during esca pathogenesis.

In this context, we hypothesized a strong interaction between esca and drought, which both affect xylem water transport. Drought events cause yield decline, and when severe and/or prolonged, vine mortality (15, 16). Due to their climatic and edaphic environment, most of the world's wine regions are exposed to a high risk of drought, as irrigation is not a sustainable long-term solution and rainfall is often not sufficient to supply grapevine evapotranspiration [e.g., in the Mediterranean area (17, 18)]. Because both drought and esca are associated with xylem hydraulic failure (13, 14, 19) and, theoretically, with nonstructural carbohydrate (NSC) consumption (1, 3, 8), these stresses could synergize and amplify the current vineyard decline. Therefore, there are real and urgent concerns regarding the outcome of the interaction between drought events and vascular pathogenesis in the grapevine.

On some levels, plant responses to vascular disease and drought appear similar and include decreases in leaf gas exchange (20–22), losses of hydraulic conductivity (14, 23, 24), wilting (i.e., decreases in cell turgor), and scorching of leaves (12, 25, 26). Because they induce similar plant responses, it could be assumed that their interactions would be synergistic. However, we lack the detailed whole-plant physiology studies necessary to determine if this is true. This is probably because

Significance

The world is witnessing a sharp increase in perennial plant dieback. The hypothesized cause is that environmental stresses such as drought are interacting with pathogens fueling plant decline. Global viticulture has seen similar decreases in fruit yield and vine longevity. One of the hypothesized causes is a synergy between drought and the grapevine vascular disease esca, for which there is no known curative treatment. In sharp contrast to this theory, our study demonstrates that drought completely suppresses esca leaf symptoms, and although esca and drought both alter plant water transport and carbon balance, they do so in completely distinct ways. This understanding reveals the complexity and unpredictability of the stress interactions thought to drive plant mortality.

Author contributions: G.B., G.A.G., and C.E.L.D. designed research; G.B., C.C., S.D., E.F., N.F., Y.G., J.J., P.L., and C.E.L.D. performed research; G.B., G.A.G., and C.E.L.D. analyzed data; and G.B., G.A.G., and C.E.L.D. wrote the paper.

The authors declare no competing interest.

This article is a PNAS Direct Submission. L.S.S. is a guest editor invited by the Editorial Board.

Published under the PNAS license.

[1]To whom correspondence may be addressed. Email: chloe.delmas@inrae.fr.

This article contains supporting information online at http://www.pnas.org/lookup/suppl/doi:10.1073/pnas.2112825118/-/DCSupplemental.

Published October 21, 2021.

www.manaraa.com

studying disease–drought interaction can be extremely challenging. Some vascular diseases, including esca, cannot be reproduced through the artificial inoculation of plants. Thus, studies rely on naturally infected field experimentation in which the disease history of specific plants is largely unknown and applying well-controlled water deficits (WD) (as well as controlling other environmental factors) is either difficult or impossible.

The main objective of this study was to explore the interaction between esca and drought and to disentangle the whole-plant physiological response to the two stresses. We overcame the technical barriers by transplanting naturally infected plants with known disease histories from the field into pots to precisely manipulate their watering regime and study the combined effect of esca and drought. We maintained half of the plants under a WD at a predawn water potential (Ψ_{PD}) ~ −1 MPa during 3 mo in two consecutive seasons, which simulated a moderate to severe level of drought (27). During these periods, we quantified plant–water relations (water potential and whole-plant and leaf-stomatal conductance), carbon balance (CO_2 assimilation, chlorophyll content, and NSC quantification in leaves and stems), and the development of esca symptoms. Our results showed that whole-plant physiological responses to esca or drought are not driven by the same underlying mechanisms; once combined, the two stresses strongly and antagonistically interact, opening perspectives on the plant–pathogen–environment relationships impacting vineyard sustainability.

Results

Drought Inhibits the Formation of Esca Leaf Symptoms. During vascular diseases, WD conditions can amplify (28, 29), hinder (30, 31), or have no effect (32) on vascular pathogens. However, most of the studies examining the impact of WD on fungal infections cannot be easily interpreted because water potential values were rarely recorded; thus, in these cases, it is impossible to assess to what extent plants (and pathogens) were experiencing drought conditions. In this study, we uprooted mature (30-y-old) naturally infected plants from the field after long-term disease monitoring. We divided plants by their symptom history record: plants that never expressed esca leaf symptoms (previously asymptomatic [pA]) and plants that expressed esca leaf symptoms at least once since 2012 (previously symptomatic [pS]). From July to October (2018 and 2019), we monitored esca leaf symptom development on all plants while we subjected half of the plants to WD, targeting a moderate to severe level of stress (Ψ_{PD} ~ −1 MPa) and maintained the well-watered (WW) plants at high Ψ_{PD} (close to 0 MPa) independently of their disease status (Fig. 1*A*). The same plants were subjected to WD each year. In both years, we observed that ~30% of WW plants developed esca leaf symptoms, while WD totally inhibited esca leaf symptom development, as none of the droughted plants developed leaf symptoms in either year (Fig. 2). More specifically, in 2018, 14% of the pA plants (WW-pA) and 50% of the pS plants (WW-pS) expressed esca leaf symptoms (Fig. 2). In 2019, 33% of WW-pA and 31% of WW-pS plants expressed esca leaf symptoms. In contrast, the totality of plants subjected to WD remained asymptomatic during the 2 y, independently of the disease status during the previous seasons (pA or pS; Fig. 2). Given the observed frequencies of symptom development in the WW-pA and WW-pS plants over the 2 y, the likelihood of having no plants express symptoms during the 2 y was less than 1 in 100 million. Moreover, esca symptom incidence found in WW plants is similar to field observations in the parcel from which the plants were transplanted. For the period from 2013 to 2017, we found an average (± SE) esca incidence of 39.5 ± 7%; more specifically, mean esca incidence in this parcel was 12.4 ± 3% for pA plants (i.e., plants that expressed esca for the first time each year) and 54.2 ± 10% for pS plants (plants that already expressed esca). To better understand the whole-plant physiological thresholds underlying each stress, we explored how plant–water relations and carbon balance changed under drought or esca at the whole-plant scale.

Water Potential Dynamic during Esca Pathogenesis Was Similar to Control WW Conditions, Not to Drought. During vascular pathogenesis, it has been found that *Verticillium* infection caused a decrease in minimum water potential (33), inducing a drought-like event. During esca, only one study found that stem water potential was not different between esca and asymptomatic plants (34); however, water potential regulation (disentangling Ψ_{MD} and Ψ_{PD}) has never been investigated during esca leaf symptom development. Applying the theoretical hydraulic model in plant water movement (35), we hypothesized that the loss in hydraulic conductivity observed during esca (13, 14) would induce an increase in xylem tension (i.e., decrease in minimum water potential) in symptomatic plants in order to maintain the

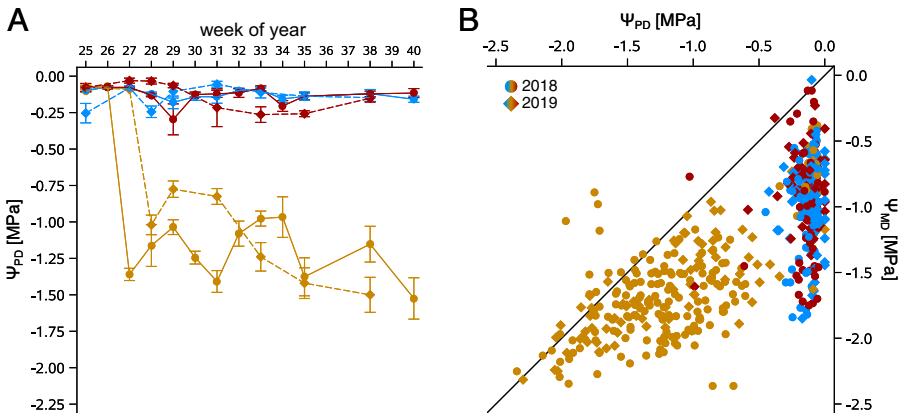

Fig. 1. Leaf water potential (Ψ) monitoring in 2018 and 2019 in *V. vinifera* cv. Sauvignon blanc. (*A*) Mean ± SE Ψ_{PD} values over the experimental periods, expressed in week of year from mid-June (week 25) to the beginning of October (week 40). Symbols and lines represent the year: circles and solid lines for 2018, diamonds and dashed lines for 2019. Colors represent the different stresses: blue for control, red for esca symptomatic, and yellow for plants under WD. (*B*) Relationship between Ψ_{PD} and midday water potential Ψ_{MD} over the 2 y; colors and symbols are the same as in *A*. The black line indicates the 1:1 regression. A general effect of the treatment (i.e., control, esca, and WD) was found for Ψ_{PD} ($F_{2,559}$ = 230.55, $P < 0.0001$) and Ψ_{MD} ($F_{2,456}$ = 126.16, $P < 0.0001$) using independent mixed linear general models fitting a normal distribution, treating the sampling date as a fixed effect and plant as a random effect. In both cases (Ψ_{PD} and Ψ_{MD}), water potentials measured in control and esca plants were similar ($P = 0.68$ and $P = 0.46$), while WD presented significantly different water potential values compared to control ($P < 0.0001$) and esca ($P < 0.0001$) using Tukey's post hoc comparisons.

www.manaraa.com

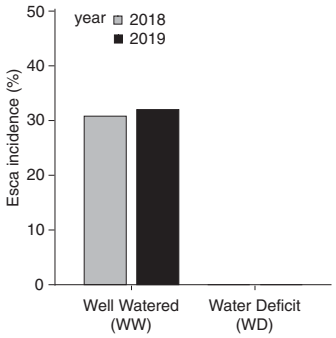

	Well-watered (WW)		Water deficit (WD)	
	pA	pS	pA	pS
Esca leaf symptom incidence in 2018	14% (2/14)	50% (6/12)	0% (0/13)	0% (0/12)
Esca leaf symptom incidence in 2019	33% (4/12)	31% (4/13)	0% (0/13)	0% (0/13)

Fig. 2. Effect of the watering regime on esca leaf symptom development in *V. vinifera* cv. Sauvignon blanc. Bars represent the seasonal esca incidence in 2018 (gray) and in 2019 (black) in WW (mean $\Psi_{PD} > -0.3$ MPa) and WD (mean $\Psi_{PD} < -0.5$ MPa from July to October) plants, pooling the historical esca records together (pA and pS as presented in the table on the right). The table shows the incidence of esca leaf symptoms in the year of experimentation (2018 or 2019). In the table, the plants are grouped by their watering regime (WW and WD plants) and by their disease history between 2012 and the year before the experimentation: plants that never expressed symptoms (pA) and plants that have expressed symptoms at least once (pS). Ratios present the number of symptomatic plants the year of experimentation in each category over the total number of plants of the category in each of the two different years.

same transpiration rate in leaves. Our results showed that midday leaf water potential (Ψ_{MD}) was not significantly different between WW control and esca-symptomatic plants (Ψ were always measured in asymptomatic leaves) over two consecutive years and was significantly lower after applying WD (Fig. 1*B*). This indicates that, contrary to what we expected, esca-symptomatic plants were able to regulate their water potential similarly to control in asymptomatic leaves (i.e., without visual symptoms). However, in 4 out of 111 Ψ_{PD} measurements, symptomatic plants presented $\Psi_{PD} < -0.5$ MPa, and in many cases, when we measured Ψ in symptomatic leaves, values were not reliable, as gel, not water, was observed exuding from petioles. This suggests that the disease leads to water transport impairment in leaves when symptoms are present and, in some rare cases, also in asymptomatic leaves. In these cases, we suspected that the occlusions inside xylem vessels induced a hydraulic disconnection between the soil (at field capacity) and the leaf. Given that esca has been shown to decrease leaf transpiration rates (20, 36), we hypothesized that changes in stomatal conductance and/or leaf canopy surface contribute to the maintenance of a sufficient water supply resulting in water potential values similar to control plants.

Drought and Esca Caused Different Dynamics in Whole-Plant and Leaf Gas Exchange. During drought, stomatal closure results from decreases in xylem water potential and an accumulation of abscisic acid in leaves (37). This mechanism prevents plants from excessive water loss and xylem embolism (38). A decrease in leaf gas exchange has also been observed during vascular diseases (refs. 20 and 21, among others), but the underlying mechanisms are still unknown. Currently, there are two prevailing hypotheses: 1) pathogen- and/or plant-derived vascular occlusions decrease hydraulic conductivity inducing stomatal closure (21, 33); or 2) pathogen-derived toxins and/or elicitors cause cellular death, loss in photosynthetic efficiency, and a subsequent decrease in gas exchange (39, 40). To test how grapevines control their stomatal conductance and transpiration during esca leaf symptom development and compare this with water deficit, we placed 20 plants in a mini-lysimeter greenhouse in order to continuously measure transpiration and determine whole-plant stomatal conductance (*Gs*, Fig. 3 *A* and *B*). We also measured gas exchange (Fig. 3 *D*, *i–iii*) and chlorophyll content (Fig. 3 *D*, *iv*) at the leaf level.

For two consecutive years, we observed two distinct recurrent patterns of whole-plant *Gs* in stressed plants, one for plants under water deficit, the other for plants presenting esca leaf symptoms (Fig. 3*A*; note that day 0 is specific for each plant and corresponds to the first day of water regime change during drought or to the day on which the first symptomatic leaf appeared during esca pathogenesis).The seasonal *Gs* dynamic in control plants (around the average of 141.18 mmol $\cdot$ m^{-2} $\cdot$ s^{-1} in Fig. 3*A*) is presented in *SI Appendix*, Fig. S1. We observed, as expected, that before imposing a different watering regime, all plants presented *Gs* similar to controls (Fig. 3 *A*, *I*). Once the watering regime changed until 12 d after the change, total *Gs* decreased, reaching a minimum average of 17.7 mmol $\cdot$ m^{-2} $\cdot$ s^{-1} (Fig. 3 *A*, *II*). Afterward, *Gs* stabilized at five times lower relative to control plants (Fig. 3 *A*, *III*). In esca-symptomatic plants, we observed that *Gs* followed (for every plant) the same pattern relative to the onset of symptom appearance. Before leaf symptom development (when the plant is apparently healthy and asymptomatic: period I), the level of *Gs* remained similar than in control plants (Fig. 3*A*). Concomitantly with the onset of symptoms and until 12 d after symptom onset, total *Gs* decreased (Fig. 3 *A*, *II*). Average *Gs* during period II for plants exhibiting symptoms was greater than WD plants, attaining a minimum daily average of 70.8 mmol $\cdot$ m^{-2} $\cdot$ s^{-1}. However, 4 out of 10 plants reached *Gs* values similar to plants under WD ($\sim$30 mmol $\cdot$ m^{-2} $\cdot$cs^{-1}, Fig. 3*A*). Later (i.e., after 13 d from the first leaf symptom appearance: period III), *Gs* recovered, raising to an average value of 103.8 $\pm$ 2.2 mmol $\cdot$ m^{-2} $\cdot$ s^{-1}. Similar to *Gs* dynamics, we found that the whole-plant maximal transpiration (E_{MAX}) sensibility to vapor pressure deficit (*D*) of esca plants was similar to controls (i.e., highly sensible) in periods I and III, while it was similar to WD (i.e., not sensible) in period II (*SI Appendix*, Fig. S2).

During WD, we observed that the reduction of *Gs* in periods II and III corresponded to the decrease in soil water potential. Likewise, whole-plant Gs_{MAX} (i.e., hourly maximum *Gs* value of the day) decreased with decreases in Ψ_{MD} under WD ($P < 0.0001$, $R^2 = 0.40$; Fig. 3*B*), especially below -1 MPa. However, esca exhibited the opposite response with Gs_{MAX} increasing with decreasing Ψ_{MD} (measured on asymptomatic leaves; $P < 0.0001$, $R^2 = 0.41$; Fig. 3*B*). This result indicates that in WW esca plants, even when Ψ_{MD} reaches fairly negative values (i.e., -1 MPa and below), nonsymptomatic leaves are receiving an ample water supply to sustain gas exchange and do not need to regulate their stomatal conductance.

During esca, the *Gs* drop in period II corresponded strongly with a decrease in the functional canopy (Fig. 3 *C*, *i*). We showed that during period II, the green canopy surface area decreased linearly over time (Fig. 3*C*), and this decrease was strongly correlated with the decrease in *Gs* ($P < 0.0001$, $R^2 = 0.65$; Fig. 3 *C*, *i*). The following recovery in *Gs* and sensibility to *D* (in period III) was probably due to the growth (and activity) of new asymptomatic leaves at the top of symptomatic shoots (one example in *SI Appendix*, Fig. S3), as we observed an

www.manaraa.com

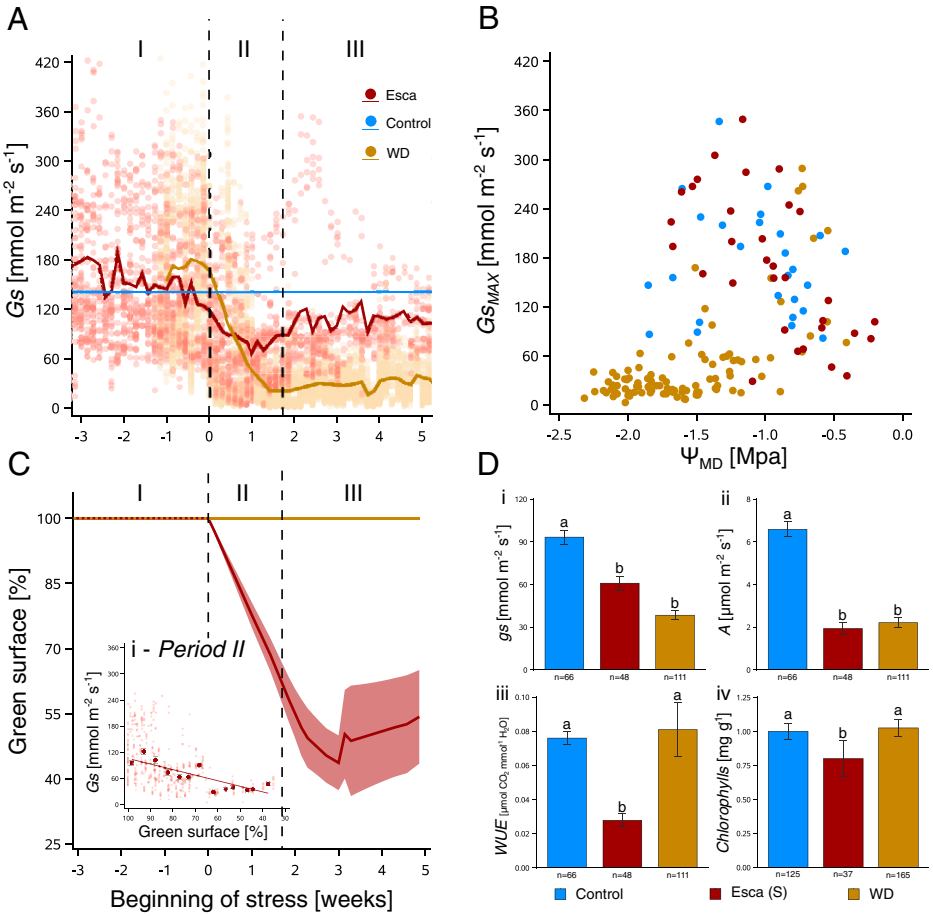

Fig. 3. Whole-plant and leaf physiology during esca and WD in *V. vinifera* cv. Sauvignon blanc: whole-plant stomatal conductance (*A*–*C*), leaf gas exchange and leaf chlorophyll content (*D*). (*A*) Evolution of the whole-plant stomatal conductance *Gs* (mmol · m^{-2} · s^{-1}) relative to the beginning of stress in weeks (i.e., week 0 indicates the first apparition of leaf symptoms or the day we changed the watering regime). Colors represent the different stresses: blue for control, red for esca leaf symptoms, and yellow for WD. The light blue line represents the average value of *Gs* in control plants over the two seasons (n = 7 plants). Dots represent hourly whole-plant *Gs* for each stressed plant, and the thick (red and yellow) lines represent the 5-d moving average of *Gs* values for symptomatic (n = 11 plants) and WD (n = 20 plants). The vertical dotted lines separate three different time periods of esca symptom and WD development (see *Drought and Esca Caused Different Dynamics in Whole-Plant and Leaf Gas Exchange*). (*B*) Relationship between midday water potential (Ψ_{MD}) and the maximum hourly *Gs* recorded on the same day (Gs_{MAX}) for different stresses. Colors are the same as in Fig. 2*A*. (*C*) Evolution in the percentage of green canopy area (green surface) relative to the beginning of stress during esca (red line) and WD (yellow line). Lines represent the average value, and the shaded band represents the SE. (*C*, *i*) Relationship between *Gs* and green surface during period II for esca-symptomatic plants. Dots represent hourly *Gs*, dark dots average Gs value in a 5% window of green surface (e.g., the first dark dot represents average *Gs* between 100% and 95% of green surface, the second between 95% and 90%). The red line represents the linear regression of the average value. (*D*, *i*) Leaf-stomatal conductance (*gs*, mmol · m^{-2} · s^{-1}). (*D*, *ii*) Net CO_2 leaf assimilation (*A*, µmol · m^{-2} · s^{-1}). (*D*, *iii*) $WUE = A \cdot gs^{-1}$, µmol · $mmol^{-1}$. (*D*, *iv*) Total chlorophyll content (a + b, mg · gFW^{-1}) for control (blue), esca-symptomatic (red), and WD (Ψ_{PD} < −0.5 MPa, yellow) leaves. Bars represent means, error bars SE, and letters indicate statistical significance (P < 0.05) from independent mixed linear general models with Tukey post hoc comparisons (*SI Appendix*, Table S1). Sample sizes (n) are presented below each bar.

increase of green canopy (Fig. 3*C*) and total leaf surface (after day 230 in *SI Appendix*, Fig. S4).

At the leaf level, we observed that the gas exchange (*gs*, *A* [assimilation], and *WUE* [water use efficiency]) and the chlorophyll content remained similar between control and asymptomatic healthy leaves from esca plants throughout the season (*SI Appendix*, Fig. S5), confirming the hypothesis that esca affects the vine physiology only after expressing the visual symptoms. Regarding the comparisons between esca-symptomatic, control, and WD leaves, we observed that leaves from control plants presented a significantly higher stomatal conductance (*gs*) than esca-symptomatic and WD leaves (Fig. 3 *D*, *i* and *SI Appendix*, Table S1). For net CO_2 assimilation (*A*, Fig. 3 *D*, *ii* and *SI Appendix*, Table S1), control leaves presented higher values than esca-symptomatic and WD leaves. Although *A* and *gs* were reduced during both esca leaf symptom development and WD, the quantity of assimilated CO_2 relative to the H_2O loss was different. Consequently, *WUE* was only reduced in esca-asymptomatic leaves, (Fig. 3 *D*, *iii* and *SI Appendix*, Table S1). Confirming that photosynthesis was more affected in esca-symptomatic leaves than in WD leaves, we observed that the total chlorophyll content was significantly lower in esca-symptomatic leaves (Fig. 3 *D*, *iv*). Esca and WD both significantly affected whole-plant *Gs* but with very different seasonal dynamics, gas exchange, and photosynthetic activity at the leaf level. Given these differences, we explored the consequences on NSC production and storage.

NSC Storage and Balance during Esca and Drought. Pathogens and drought may cause an imbalance in carbon status by variously affecting photosynthesis and growth (1). Thus, at the start of the stress period or when stress is moderate, photosynthesis is usually less affected than growth, which leads to the accumulation of sugars (41). However, when the stress is prolonged or becomes

www.manaraa.com

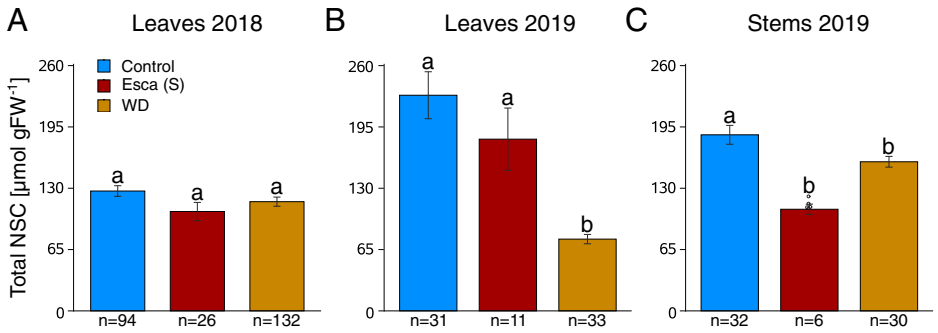

Fig. 4. Total NSC content in µmol · gFW^{-1} over the 2 y for control (blue), esca-symptomatic (red), and WD (Ψ_{PD} < −0.5 MPa, yellow) leaves and stems. (*A*) Mean NSC content in leaves in 2018. (*B*) Mean NSC content in leaves in 2019. (*C*) Mean NSC content in stems in 2019. Bars represent means and error bars SEs; letters indicate statistical significance (P < 0.05) from independent mixed linear general models with Tukey's post hoc comparisons (*SI Appendix*, Tables S2 and S3). Sample sizes (*n*) are presented below each bar, and individual data points (dots) are presented for bars with sample sizes ≤10.

severe, photosynthesis is in turn inhibited, eventually causing the depletion of stored NSC, thereby accelerating plant decline. Also, vascular pathogens could reduce photosynthetic activity by causing cellular/leaf death, actively consume NSC for their survival, induce C-expensive plant defenses, and indirectly interfere with phloem transport when they generate xylem hydraulic failure (3). In order to understand how esca and WD affect the carbon (im)balance, NSC were quantified in annual organs (leaves) during summer 2018 and 2019 and in perennial organs (stems of the current year) in winter (January 2019) and summer 2019 (Figs. 4 and 5 and *SI Appendix*, Figs. S6–S9 and Tables S2 and S3).

Strikingly, none of the treatments induced severe carbon depletion, as the NSC levels were always relatively high [comparing our results to different NSC quantifications (42)]. It is important to note that in these grapevines, fruit clusters were removed right after budbreak, so crop load differences would not influence the NSC content in our samples. In 2018, we observed that all leaves (from control, symptomatic, or WD plants) presented the same content of total NSC (around 130 µmol · g fresh weight (gFW^{-1}); Fig. 4*A* and *SI Appendix*, Table S2). In 2019, total NSC content in leaves was significantly decreased only by WD conditions (Fig. 4*B* and *SI Appendix*, Table S2). In 2019, control stems presented a significantly higher NSC content (186.6 ± 10 µmol · gFW^{-1}, on average) compared to the other stems (Fig. 4*C* and *SI Appendix*, Table S3). In 2019, we observed an opposite NSC distribution between leaves and stems (Fig. 4 *B* and *C*) depending on the stress: control and esca-symptomatic plants presented higher NSC content in leaves than in stems, while during WD (second year), NSC content was higher in stems than leaves. This result could indicate that esca and WD differently affect primary metabolism and carbohydrate storage dynamics.

Partitioning the different carbohydrates, we observed different dynamics for esca and WD (Fig. 5 and *SI Appendix*, Figs. S6–S9 and Tables S2 and S3). Esca-symptomatic and WD leaves accumulated high levels of hexoses (glucose and fructose) during both years (two to five times higher compared to controls, except for glucose during WD in 2019, Fig. 5 *A* and *B* and *SI Appendix*, Table S2). Sucrose content was significantly lower for esca-symptomatic leaves (0.5 times compared to controls both years), while it was similar to (or slightly lower than) control during WD (Fig. 5 *A* and *B*). Confirming this trend, we found that hexoses and sucrose in leaves exhibited opposite relationships when related to leaf symptom severity in which glucose and fructose significantly increased, while sucrose significantly decreased with symptom severity (i.e., percentage of green leaf tissue; *SI Appendix*, Fig. S7). Starch was significantly lower during both stresses (0.5 times lower on average), especially during the second year of WD (0.1 times compared to controls, corresponding to 9 ± 2.4 µmol · gFW^{-1}), indicating that carbon reserves were consumed (or not produced) in response to stress. In stems, we observed differences in fructose content with significantly higher levels during WD (1.5 times relative to control; Fig. 5*C* and *SI Appendix*, Table S3), suggesting that the growth inhibition leads to hexose accumulation also in perennial organs. Sucrose was significantly lower in esca-symptomatic stems (0.3 times relative to control; Fig. 5*C*), indicating that reduced phloem transport (sucrose is the mobile NSC form) or an increased invertase activity could be present in stems. During esca and WD, stems exhibited glucose and starch contents similar to (or slightly different from) controls, showing that reserve accumulation is still active during these stressing conditions (Fig. 5*C*). Asymptomatic (healthy) leaves

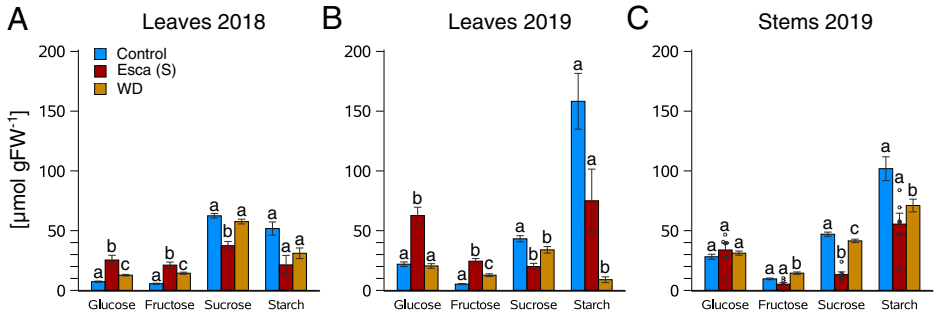

Fig. 5. Content of different NSC (glucose, fructose, sucrose, and starch) in µmol · gFW^{-1} over the 2 y for control (blue), esca-symptomatic (red), and WD (Ψ_{PD} < −0.5 MPa, yellow) leaves and stems. (*A*) Mean content in leaves in 2018. (*B*) Mean content in leaves in 2019. (*C*) Mean content in stems in 2019. Bars represent means and error bars SE, and letters indicate statistical significance (P < 0.05) from independent mixed linear general models with Tukey's post hoc comparisons. Different statistical tests were done for each different sugar (see *SI Appendix*, Tables S2 and S3 for details). Sample sizes for each bar are presented in the text and in Fig. 3, and individual data points (dots) are presented for bars with sample sizes ≤10.

www.manaraa.com

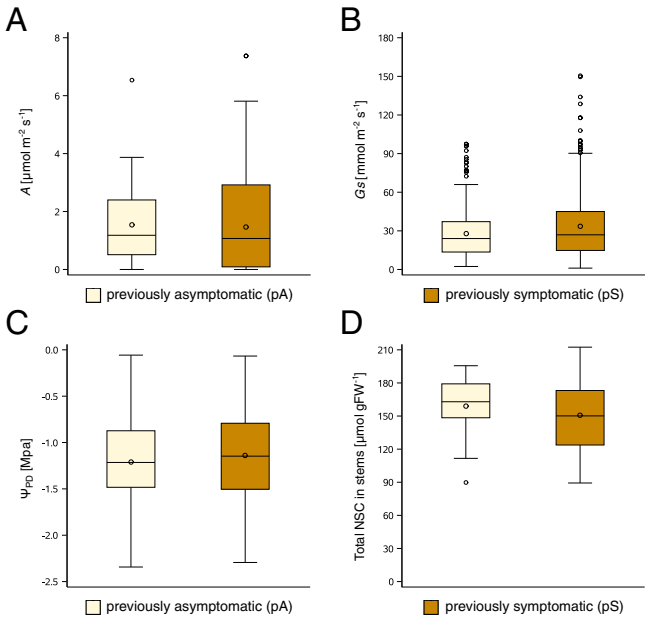

Fig. 6. Effect of disease history on plant physiological response to drought. The colors represent the absence (pA, light yellow) or presence (pS, dark yellow) of esca leaf symptoms between 2012 and 2017 in plants submitted to WD in 2018 and 2019. (*A*) CO_2 assimilation (*A*, $\mu mol \cdot m^{-2} \cdot s^{-1}$), (*B*) whole-plant stomatal conductance (*Gs*, $mmol \cdot m^{-2} \cdot s^{-1}$), (*C*) predawn water potential (Ψ_{PD}, MPa), (*D*) total NSC in stems ($\mu mol \cdot gFW^{-1}$) after changing the watering regime. The disease history (pA versus pS) had no significant effect on these or other (*SI Appendix*, Table S4) recorded variables. Boxes and bars show the medians, quartiles, and extreme values, circles within boxes correspond to means, and circles outside boxes correspond to outlier values.

and stems from esca plants presented a variable carbohydrate content (*SI Appendix*, Fig. S8). In most of the cases, they presented carbohydrate content similar to control plants, while for others (especially in the total NSC content in leaves and stems in 2019), their NSC dynamic was more similar to esca-symptomatic samples. Finally, it is worth noting that in the NSC quantification in stems during the winter 2018 to 2019 dormancy (i.e., stems produced in 2018 and sampled the next winter between the two experimental seasons), none of the quantified metabolites were significantly different compared to controls (*SI Appendix*, Fig. S9 and Table S3).

The Long-Term Esca Leaf Symptom History Did Not Impact Plant Physiological Response to Drought. We observed that drought inhibits esca leaf symptom expression (Fig. 2). We then explored whether plant response to drought differed between asymptomatic plants with contrasting disease histories (pA-pS). As presented in Fig. 6 and *SI Appendix*, Table S4, we found that the disease's historical record had no significant effect on any of the recorded variables (water potential, whole-plant and leaf gas exchange, and NSC). This result suggests that esca does not alter long-term plant susceptibility to drought. Bortolami et al. (14) observed that plants with different disease histories presented similar hydraulic integrity; here, we confirmed that esca leaf symptom development affects the plant physiology mainly during the year of expression and not over the long term. These findings can partially explain why esca-symptomatic plants can frequently appear asymptomatic during the successive seasons [as observed in field surveys (43, 44)].

Discussion

Increasing plant mortality is one of the major issues threatening perennial forestry and agricultural ecosystems. The impact of biotic–abiotic stress interactions on plant physiology certainly plays a crucial role in the extent of this mortality. Here, we studied the interaction between drought and vascular disease and the subsequent physiological consequences in the grapevine. Esca (a vascular disease) and drought are two stresses that frequently coexist in vineyards. Even though there is anecdotal evidence that hot periods could contribute to the induction of esca leaf symptom appearance (45–47), the underlying plant physiological status has still never been detailed during these events, leaving many doubts about how drought and esca interact.

We demonstrated that prolonged WD conditions (at $\Psi_{PD} \sim -1$ MPa for 3 mo) totally inhibited esca leaf symptom development. At the same time, plant disease history (i.e., esca leaf symptom expression over several years) had no impact on plant response to drought. Under the drought condition applied, plant transpiration was low while hydraulic integrity was preserved (*SI Appendix*, Figs. S3 and S10). The most prominent hypothesis of esca leaf symptom formation states that toxins (or elicitors) are transported from pathogen niches in the trunk to leaves through the transpiration stream (8). The drought–esca antagonism suggests that 1) transpiration is a key mechanism driving esca leaf symptom expression and that 2) drought could trigger systemic responses that might interfere with pathogenicity (e.g., reducing fungal toxic activities) and/or enhance plant defenses (e.g., accumulation in soluble sugars and phenolic compounds). The clear antagonism between esca and drought strengthens the importance of integrative studies (i.e., monitoring plant physiology under multiple stresses) to understand the role of climate in perennial plant decline. We highlighted the need to determine the physiological thresholds triggering different plant responses to stress if we are to understand and predict the impact of climate change on agroecosystems. Interpreting our results, we could expect that future climate change could lead either to a decrease in esca incidence if Ψ_{PD} reaches low values (around −1 MPa) or an increase in esca incidence if the vapor pressure deficit increases but water availability remains sufficient to sustain high transpiration. Moreover, other practices, such as irrigation, that can temporarily mitigate WD could accelerate vine decline by esca. In this context, changing cultural practices in the absence of a complete understanding of biotic–abiotic interactions and the different physiological thresholds contributing to plant mortality could lead to unforeseen outcomes.

Esca and drought primarily affect the same plant tissue: the xylem vasculature. This simple fact, coupled with other similarities between the phenology of these stresses, have led many authors to hypothesize that vascular pathogens and WD induce the same mechanisms prior to plant death (2, 33). Our results largely reject this hypothesis, finding that the two stresses induced distinct physiological responses. We demonstrated in previous work that esca pathogenesis is associated with hydraulic failure caused by vascular occlusion (13, 14), which contrasts with the cavitation-induced hydraulic failure during drought (48). Here, we showed that esca never caused any significant changes in the water potential gradient during our 2-y study. This result can be explained by the observation of whole-plant stomatal conductance. *Gs* decreased during esca leaf symptoms (as during WD in period II; Fig. 3*A*), but it was directly correlated with the percentage of symptomatic leaves (percent of the total plant canopy), not by a change in soil (i.e., predawn) water potential as during drought. Consequently, as stomatal conductance decreased linearly with esca leaf symptom development, the remaining functional (i.e., nonoccluded) xylem vessels sustain sufficient water transport to nonsymptomatic leaves, which function similarly to controls. Interestingly, we observed that 2 to 3 wk after the first apparition of leaf symptoms, on top of symptomatic shoots, new asymptomatic shoots grew and that

www.manaraa.com

Gs recovered to a level close to control plants. Confirming this trend, we observed that at the whole-plant scale, transpiration sensibility to vapor pressure deficit was similar to WD conditions only during esca leaf symptom formation (i.e., in period II; *SI Appendix*, Fig. S2) and that asymptomatic regrowth was able to restore whole-plant transpiration rates equivalent to controls in period III. In vineyards, grapevines are often continuously trimmed during summer to control canopy size; thus, only one study reported asymptomatic regrowth in the field after extreme esca leaf symptom development (47). In the future, new attention should be given to how asymptomatic regrowth could restore (or mitigate) the negative effects of esca symptoms on berry quality and reserve synthesis. For example, our study showed that esca did not influence stem starch content in winter [*SI Appendix*, Fig. S9, contrasting from Petit et al. (36)]; this could be due to the presence of new asymptomatic leaves that helped maintain starch reserves as in control plants.

Measurements at the leaf level showed that the photosynthetic apparatus is more compromised during esca than during drought. This result could support two hypotheses: 1) a toxic molecule, produced by the pathogens in the trunk and transported by the xylem, could interfere with the leaf functioning, and/or 2) hydraulic failure (13, 14) might impair phloem transport, causing a subsequent accumulation of hexoses in leaves and a down-regulation of leaf *A* and *gs*. Indeed, esca-symptomatic leaves and stems consistently exhibited lower sucrose concentrations (the main sugar transport form) and higher hexose content, suggesting that carbohydrate efflux from leaves would be reduced during esca and the invertase activity enhanced. It has been shown that the accumulation of hexoses and/or the increased ratio of hexoses to sucrose during biotic stress could stimulate genes related to plant defense and accelerate leaf senescence (49). Therefore, both toxic metabolites and hydraulic failure (loss of hydraulic conductance) could contribute to leaf senescence and esca symptom formation.

In conclusion, even if esca and drought were antagonistic when applied simultaneously, and if esca had no long-term impact on drought susceptibility, both stresses negatively impacted perennial organs and plant physiological functioning (although in distinct ways). Consequently, drought and vascular disease could act synergistically over the longer term, contributing together to plant decline.

Materials and Methods

Plant Material and Esca Symptom Notation. The grapevine variety Sauvignon blanc (*Vitis vinifera*), grafted onto 101-14 Millardet et de Grasset (101-14 MGt), was planted in 1992 at INRAE Nouvelle-Aquitaine Bordeaux (44°47′24.8″N, 0°34′35.1″W). Following the protocol from Bortolami et al. (13), plants ($n = 51$) were uprooted in winter 2018 and transferred into 20-L pots, allowing environmental and physiological monitoring. During the two experimental seasons (2018 and 2019), fruits and secondary shoots were removed just after budbreak. In the greenhouse, plants were irrigated with nutritive solution (0.1 mM $NH_4H_2PO_4$, 0.187 mM NH_4NO_3, 0.255 mM KNO_3, 0.025 mM $MgSO_4$, 0.002 mM Fe, and oligoelements [B, Zn, Mn, Cu, and Mo]); climatic conditions were monitored every 15 min using temperature and humidity probes (S-THB-M002, Onset) and global radiation sensors (S-LIx-M003, Onset) connected to a data logger (U300-NRC, Onset). From 2012, the development of esca leaf symptoms for all plants was monitored in the vineyard (2012 to 2017) and in the greenhouse (2018 to 2019) following Lecomte et al. (12) to classify the plants as asymptomatic or esca symptomatic every year. Before the experiment started (May 2018), each plant was classified by its disease historical record: plants that never expressed symptoms since 2012 (pA) and plants that expressed symptoms at least once since 2012 (pS). During the 2 y of experimentation, the appearance of leaf symptoms was checked twice per week (from June 2018 to October 2019) on every plant. Consequently, each sample (leaf or stem) was classified by both a general disease status of the whole plant and of the specific collected organ: samples from control plants (i.e., asymptomatic from June to October), asymptomatic samples from symptomatic plants (both before and after symptom appearance), and symptomatic (presenting tiger-stripe leaves) samples. One example of esca symptom appearance and evolution is presented in *SI Appendix*, Fig. S3. To test for the presence of esca-related vascular pathogens in these plants, we detected and quantified, at the end of the experimentation, the DNA of two ascomycete pathogens (*Phaeomoniella chlamydospora* and *Phaeoacremonium minimum*) in the trunk of 24 plants among the 51 (see the method and results in *SI Appendix*, Method S1 and Table S5).

Balance Data Analysis. From mid-June to October (in 2018 and 2019), a subset of plants ($n = 20$) was placed in a mini-lysimeter greenhouse phenotyping platform (Bord'O platform, INRAE Bordeaux) in which pots were continuously weighed on individual scales (CH15R11, OHAUS type CHAMP). The pots were placed into dark plastic bags well fixed around the trunk to prevent water loss by soil evaporation. The whole-plant transpiration E (mmol · s^{-1} · m^{-2}) was calculated as follows:

$$E = \frac{\Delta_w}{A_L} \times \frac{1}{MW_w}, \quad [1]$$

where Δw corresponds to the weight changes during every hour (grams per second), A_L to the total leaf area of the plant (square meters), and MW_w to the molecular weight of water (18 g · mol^{-1}). Δw was considered only when not aberrant (i.e., between 0 and −0.5 kg · h^{-1}). Moreover, to avoid rarely recorded Δw, extreme outlier values (i.e., values three times lower than the lower quartile or three times higher than the highest quartile) were removed for each day and plant. Total leaf area (A_L) was estimated through the relationship obtained between the leaf midrib length and the leaf surface (measured with a leaf area meter: LI-3000, LI-COR) for ∼150 leaves. Leaf midribs were measured on all the leaves of each plant every week in 2018 and every other week in 2019 and, in case of esca symptom presence, every leaf was noted as asymptomatic, esca-symptomatic, or from asymptomatic regrowth. In the majority of symptomatic plants, 5 to 15 d after leaf symptoms appeared, new green shoots grew from the secondary buds: they were noted as "asymptomatic regrowth" (e.g., *SI Appendix*, Fig. S3). In order to obtain a daily constant change in leaf area, a linear increase (or decrease) was interpolated between each measure of leaf area. Likewise, a constant change in the percentage of symptomatic leaves was interpolated between each measure. The whole-plant stomatal conductance *Gs* (millimoles per second per square meter) was calculated as follows:

$$G_s = K_G(T)\ x\ \frac{E}{D}, \quad [2]$$

where $K_G(T)$ corresponds to the conductance coefficient (kPa · m^3 · kg^{-1}), E to the transpiration, and D to the vapor pressure deficit (kPa) calculated using relative humidity (%) and T (°C) from climatic records (50). To avoid errors in *Gs* estimations, values were used for analysis only when D was >0.6 kPa (51) and light conditions were saturating for photosynthesis (>700 μmol · m^{-2} · s^{-1} photosynthetic photon flux density).

WD Treatment and Maintenance. At the beginning of the two seasons, every plant was watered at its maximum capacity and left to drain water excess for half a day. The resulting weight was taken as field capacity, and WW plants were irrigated to this weight every other day. The average watering volume from the plants on the scales was used to water the remaining plants that were not on the balances. WD was induced on 25 (over 51) plants for two consecutive seasons (the same plants were subjected to water deficit in 2018 and 2019 from July to October), and the other 26 plants were kept under WW conditions. Among these plants, the 20 placed on the scales were half WW and half under WD. At the beginning of the experimentation in 2018, half of the WD plants had never expressed esca leaf symptoms since 2012 (pA), while the other half expressed symptoms at least once in the past (pS). Similarly, 14 out of the 26 plants under the WW regime were previously asymptomatic (Fig. 2). On the first of July 2018 and 2019, we stopped watering the plants. WD plants were maintained for a period of 3 mo (from July to October 2018 and 2019) at a target weekly average Ψ_{PD} between −0.6 and −1.7 MPa, with outliers below or above these thresholds representing 20% of the values (*SI Appendix*, Fig. S11). These conditions are sufficient to reduce plant transpiration without decreasing stem hydraulic conductivity in the grapevine (27). We checked Ψ_{PD} with a Scholander pressure chamber (Precis 2000) on three up to five plants every other day and every day on two plants with stem psychrometers (ICT International). Placed in a central internode of a stem of the current year, the psychrometers record the stem water potential (Ψ_{Stem}) every 30 min. Once Ψ_{PD} reached an average of −1 MPa, we noted the exact weight for the 10 plants placed on the scales (see *Balance Data Analysis*). These plants were then watered with nutritive solution every 3 d (and at necessity when Ψ_{PD} dropped below −1.5 MPa) at this weight until the end of the experiment (beginning of October). The average watering volume from these plants was used to water

www.manaraa.com

the remaining 15 WD plants that were not on the balances. During the whole experiment, we watered WD plants with 0.1 to 0.6 L every 3 d in pots with a pot capacity between 6 and 8 L (i.e., approximately from 1 to 10% of the field capacity).

Hydraulic Integrity and Water Potential Analysis. To check the effect of WD on the hydraulic integrity of the perennial organs, in 2019, we measured stem specific hydraulic conductivity (k_s) and stem theoretical hydraulic conductivity (k_{th}) in 73 different stems (39 control and 34 from WD plants) over nine sampling dates (*SI Appendix*, Fig. S10) as explained in Bortolami et al. (14). Water potential was monitored in at least 25 plants per date (every week in 2018 and every other week in 2019) from June to October in 2018 and 2019. We measured Ψ (both Ψ_{PD} and Ψ_{MD}) on 26 different dates, corresponding to 632 measures in control (asymptomatic WW) plants, 213 in esca-symptomatic plants, and 650 in WD plants. Every water potential measurement was done on mature leaves with a Scholander pressure chamber. Ψ_{PD} was measured between 4:00 and 6:00 AM, Ψ_{MD} on well-exposed leaves between 1:00 and 3:00 PM. Regarding esca-symptomatic plants, water potentials were measured only on asymptomatic (green) leaves. The presence of gel and tyloses in the xylem vessels of symptomatic leaves [demonstrated by Bortolami et al. (13)] made the detection of water potential with the pressure chamber difficult (and sometimes impossible). Sometimes gel (and not water) was rapidly exuded from the petioles at high Ψ (~0 MPa), and sometimes it appeared at low Ψ (between -1 and -3 MPa) or did not appear at all (<-7 MPa). However, in asymptomatic leaves, gel was not detected during Ψ measurements; therefore, the values should reflect the water status of the plant.

Gas Exchange Analysis. Once per week from June to October 2019, maximal leaf gas exchange measurements were registered between 9:00 AM and 12:00 PM on mature well-exposed leaves using the TARGAS-1 portable photosynthesis system (PP Systems). Optimal conditions of photosynthetic active radiation were set in the cuvette (1,500 $\mu mol \cdot m^{-2} \cdot s^{-1}$). The following parameters were recorded on each leaf: stomatal conductance, *gs* (millimoles per second per square meter); CO_2 assimilation, *A* (micromoles per second per square meter); water use efficiency, *WUE* (= *A*/*gs*) (micromoles of CO_2 per millimole of H_20). In some cases, the level of CO_2 absorbed (*A*) by the leaf was negative. In these cases, *A* was either close to zero (between 0 and -1 $\mu mol \cdot s^{-1} \cdot m^{-2}$, $n = 24$, 16 water deficit and 8 esca-symptomatic) or negative (between -2 and -20 $\mu mol \cdot s^{-1} \cdot m^{-2}$, $n = 20$ esca symptomatic). We considered the first group of measures as a possible leaf respiration (at the limit of detection) and the highly negative *A* values as artifacts given by the advanced leaf destruction during symptoms. Consequently, we manually changed all these records in $A = 0$ and $WUE = 0$. However, other studies should confirm the possible high respiration (i.e., CO_2 rejection) rates during esca leaf symptoms. Measurements were performed on 50 plants on 12 different dates for a total of 290 measures (66 measures on control leaves, 65 on asymptomatic leaves on esca plants, 48 on esca-symptomatic leaves, and 111 on WD leaves). For symptomatic leaves, gas exchanges were measured on their green part as much as possible. Plants under WD were considered for analysis only when $\Psi_{PD} < -0.5$ MPa, as plants with $\Psi_{PD} > -0.3$ MPa (i.e., when every plant was still under WW conditions) presented values similar to control plants ($F_{1,13} = 0.25$, $P = 0.62$ for *A*, $F_{1,13} = 1.98$, $P = 0.18$ for *gs*).

NSC and Chlorophyll Quantification. To quantify NSC over the course of the experimentation, leaves were sampled every week in 2018 on 24 random plants (half WW and half WD) on the same day and plants we measured Ψ_{PD} and Ψ_{MD}. In 2019, leaves and stems were sampled every other week on 12 random plants (half WW and half WD), thus resulting in 25 sampling dates on 51 plants for a total of 509 samples, specifically, in 2018: 94 leaves from control plants, 66 esca-asymptomatic, 26 esca-symptomatic, and 132 WD leaves; in 2019: 31 leaves and 32 stems from control plants, 20 leaves and 10 asymptomatic stems from esca plants, 11 leaves and 6 esca-symptomatic stems, and 33 leaves and 30 WD stems. All samples (stems or leaf blades) were collected in the early morning (between 7:00 and 10:00 AM) to avoid effects of NSC diel fluctuations, directly put in liquid nitrogen, and stored at -80 °C until analysis. For stems, one internode (including wood and bark) was sampled. For leaves, the whole blade (including green and scorched areas for symptomatic leaves) was sampled. Frozen samples were ground with ball tissue lyser (GenoGrinder 2010, Spex Sample Prep, at 30 Hz for 45 s for leaves and Tissuelyser II, Qiagen, for stems). A total of 20 $\pm$ 2 mg powder was weighted into 1.1-mL micronic tubes (MP32033L, Micronic), adding approximately the same volume of polyvinylpolypyrrolidone (77627, Sigma-Aldrich) to precipitate polyphenols and avoid interaction with the enzymes used to measure NSC. Samples were randomized into 96-micronic racks (MPW51001BC, Micronic). Every rack contained a maximum of 84 samples, six empty tubes (for extraction blank), and six tubes with a biological standard (obtained by mixing the powder from different samples). Assays were performed as described in Biais et al. (52) using the Starlet pipetting robot (Hamilton). After an ethanolic extraction, we divided (from every tube) the supernatant from the pellet. Determination of chlorophyll content was adapted from Arnon (53). Immediately after extraction, 50 μL supernatant was mixed with 120 μL 98% ethanol and the absorbance was read at 645 and 665 nm in a microplate reader (SAFAS MP96). Chlorophyll content, expressed as milligrams per gram fresh weight, was calculated using the following empirical formulas:

$$\text{Chlorophyll } a = 5.21 \times A_{665} - 2.07 \times A_{645}, \quad [3]$$

$$\text{Chlorophyll } b = 9.29 \times A_{645} - 2.74 \times A_{665}, \quad [4]$$

which have been obtained by using commercial chlorophyll; A_{645} and A_{665} correspond to the two absorbances. Glucose, fructose, and sucrose, expressed as $\mu mol \cdot gFW^{-1}$, were quantified in 5 μL ethanolic supernatant, and the absorbance was read at 340 nm in MP96 microplate readers (54). For the determination of starch, expressed as $\mu mol \cdot gFW^{-1}$, the pellet was suspended in 0.1M NaOH and heated at 95 °C for 20 min and neutralized with HCl, and starch was then quantified from 5 μL supernatant and the absorbance read at 340 nm in MP96 microplate readers as in Hendriks et al. (55).

Statistical Analysis. The effect of esca leaf symptoms and WD was tested on water potential (Ψ_{PD} and Ψ_{MD}), leaf gas exchange (*gs*, *A*, *WUE*), chlorophyll content (a + b), and NSC (glucose, fructose, sucrose, starch, and total NSC) content in leaves and stems using independent mixed linear general models (one per each response variable, organ, and experimental year). The treatment (control, esca-asymptomatic, esca-symptomatic, and WD leaves) and the sampling date were entered as fixed effects (covariables), and the plant was treated as a random effect, since different leaves were sometimes analyzed from the same plant in the GLIMMIX procedure (SAS 9.4; SAS Institute), and logarithmic transformations were done when appropriate to fit normality. Specific treatments were compared using Tukey's post hoc tests adjusted for multiple comparisons. The relationships between Ψ_{MD} on Gs_{MAX} during WD and esca and between the green surface (using 5% interval average values) and *Gs* were calculated using linear regression models in the REG procedure (SAS 9.4; SAS Institute).

Data Availability. Raw datasets are available in the INRAE dataverse: https://data.inrae.fr/citation?persistentId=doi:10.15454/SHLIHA, Portail Data INRAE, V1 (56).

ACKNOWLEDGMENTS. We thank the experimental teams of UMR SAVE, UMR Biologie du Fruit & Pathologie, and UMR EGFV (Bord'O platform, INRAE, Bordeaux, France) for providing the materials and logistics. We thank Isabelle Demeaux (UMR SAVE) for providing technical knowledge and support. We thank all the people (from internships to professors) that helped with the leaf surface measurements. This work was supported by the French Ministry of Agriculture and Food, FranceAgriMer, and the Comité National des Interprofessions des Vins à appellation d'origine et à indication géographique within the PHYSIOPATH Project (22001150-1506; Program Plan National Dépérissement du Vignoble) awarded to C.E.L.D.

1. N. McDowell *et al.*, Mechanisms of plant survival and mortality during drought: Why do some plants survive while others succumb to drought? *New Phytol.* **178**, 719–739 (2008).
2. K. A. Yadeta, B. P. J Thomma, The xylem as battleground for plant hosts and vascular wilt pathogens. *Front Plant Sci* **4**, 97 (2013).
3. J. Oliva, J. Stenlid, J. Martínez-Vilalta, The effect of fungal pathogens on the water and carbon economy of trees: Implications for drought-induced mortality. *New Phytol.* **203**, 1028–1035 (2014).
4. C. D. Allen *et al.*, A global overview of drought and heat-induced tree mortality reveals emerging climate change risks for forests. *For. Ecol. Manage.* **259**, 660–684 (2010).
5. J. M. Alston, O. Sambucci, "Grapes in the world economy" in *The Grape Genome*, D. Cantu, M. A. Walker, Eds. (Springer International Publishing, 2019), pp. 1–24.
6. I. Morales-Castilla *et al.*, Diversity buffers winegrowing regions from climate change losses. *Proc. Natl. Acad. Sci. U.S.A.* **117**, 2864–2869 (2020).
7. V. Mondello *et al.*, Management of grapevine trunk diseases: Knowledge transfer, current strategies and innovative strategies adopted in Europe. *Phytopathol. Mediterr.* **57**, 369–383 (2019).
8. M. Claverie, M. Notaro, F. Fontaine, J. Wery, Current knowledge on grapevine trunk diseases with complex etiology: A systemic approach. *Phytopathol. Mediterr.* **59**, 29–53 (2020).
9. C. Bertsch *et al.*, Grapevine trunk diseases: Complex and still poorly understood. *Plant Pathol.* **62**, 243–265 (2013).
10. M. Fischer, S. P. Ashnaei, Grapevine, esca complex, and environment: The disease triangle. *Phytopathol. Mediterr.* **58**, 17–27 (2019).

www.manaraa.com

11. G. Surico, L. Mugnai, G. Marchi, Older and more recent observations on esca: A critical overview. *Phytopathol. Mediterr.* **45**, S68–S86 (2006).
12. P. Lecomte *et al.*, New insights into esca of grapevine: The development of foliar symptoms and their association with xylem discoloration. *Plant Dis.* **96**, 924–934 (2012).
13. G. Bortolami *et al.*, Exploring the hydraulic failure hypothesis of esca leaf symptom formation. *Plant Physiol.* **181**, 1163–1174 (2019).
14. G. Bortolami *et al.*, Seasonal and long-term consequences of esca grapevine disease on stem xylem integrity. *J. Exp. Bot.* **72**, 3914–3928 (2021).
15. M. M. Chaves *et al.*, Grapevine under deficit irrigation: Hints from physiological and molecular data. *Ann. Bot.* **105**, 661–676 (2010).
16. C. Van Leeuwen, P. Darriet, The impact of climate change on viticulture and wine quality. *J. Wine Econ.* **11**, 150–167 (2016).
17. H. Fraga, A. C. Malheiro, J. Moutinho-Pereira, J. A. Santos, Future scenarios for viticultural zoning in Europe: Ensemble projections and uncertainties. *Int. J. Biometeorol.* **57**, 909–925 (2013).
18. J. M. Costa *et al.*, Modern viticulture in southern Europe: Vulnerabilities and strategies for adaptation to water scarcity. *Agric. Water Manage.* **164**, 5–18 (2016).
19. G. A. Gambetta *et al.*, The physiology of drought stress in grapevine: Towards an integrative definition of drought tolerance. *J. Exp. Bot.* **71**, 4658–4676 (2020).
20. M. Magnin-Robert *et al.*, Leaf stripe form of esca induces alteration of photosynthesis and defence reactions in presymptomatic leaves. *Funct. Plant Biol.* **38**, 856–866 (2011).
21. R. Castillo-Argaez, B. Schaffer, A. Vazquez, L. D. S. L. Sternberg, Leaf gas exchange and stable carbon isotope composition of redbay and avocado trees in response to laurel wilt or drought stress. *Environ. Exp. Bot.* **171**, 103948 (2020).
22. T. Knipfer *et al.*, Predicting stomatal closure and turgor loss in woody plants using predawn and midday water potential. *Plant Physiol.* **184**, 881–894 (2020).
23. B. Choat *et al.*, Global convergence in the vulnerability of forests to drought. *Nature* **491**, 752–755 (2012).
24. J. K. Mensah, M. A. S. Sayer, R. L. Nadel, G. Matusick, L. G. Eckhardt, Physiological response of *Pinus taeda* L. trees to stem inoculation with *Leptographium terebrantis*. *Trees (Berl.)* **34**, 869–880 (2020).
25. M. K. Bartlett, T. Klein, S. Jansen, B. Choat, L. Sack, The correlations and sequence of plant stomatal, hydraulic, and wilting responses to drought. *Proc. Natl. Acad. Sci. U.S.A.* **113**, 13098–13103 (2016).
26. M. Flajšman, S. Radišek, B. Javornik, Pathogenicity assay of *Verticillium nonalfalfae* on hop plants. *Bio Protoc.* **7**, e2171 (2017).
27. G. Charrier *et al.*, Drought will not leave your glass empty: Low risk of hydraulic failure revealed by long-term drought observations in world's top wine regions. *Sci. Adv.* **4**, eaao6969 (2018).
28. L. Croisé, F. Lieutier, H. Cochard, E. Dreyer, Effects of drought stress and high density stem inoculations with *Leptographium wingfieldii* on hydraulic properties of young Scots pine trees. *Tree Physiol.* **21**, 427–436 (2001).
29. L. K. S. Silva Lima *et al.*, Water deficit increases the susceptibility of yellow passion fruit seedlings to Fusarium wilt in controlled conditions. *Sci. Hortic. (Amsterdam)* **243**, 609–621 (2019).
30. B. W. Pennypacker, K. T. Leath, R. R. Hill, Impact of drought stress on the expression of resistance to *Verticillium albo-atrum* in alfalfa. *Phytopathology* **81**, 1014–1024 (1991).
31. A. Arango-Velez *et al.*, Differences in defence responses of Pinus contorta and Pinus banksiana to the mountain pine beetle fungal associate Grosmannia clavigera are affected by water deficit. *Plant Cell Environ.* **39**, 726–744 (2016).
32. D. T. Lopisso, J. Knüfer, B. Koopmann, A. von Tiedemann, The vascular pathogen *Verticillium longisporum* does not affect water relations and plant responses to drought stress of its host, *Brassica napus*. *Phytopathology* **107**, 444–454 (2017).
33. R. L. Bowden, D. I. Rouse, T. D. Sharkey, Mechanism of photosynthesis decrease by *Verticillium dahliae* in potato. *Plant Physiol.* **94**, 1048–1055 (1990).
34. L. Andreini *et al.*, Gas exchange, stem water potential and xylem flux on some grapevine cultivars affected by esca disease. *SAJEV* **30**, 142–147 (2016).
35. M. T. Tyree, J. S. Sperry, Do woody plants operate near the point of catastrophic xylem dysfunction caused by dynamic water stress?: Answers from a model. *Plant Physiol.* **88**, 574–580 (1988).
36. A.-N. Petit, N. Vaillant, M. Boulay, C. Clément, F. Fontaine, Alteration of photosynthesis in grapevines affected by esca. *Phytopathology* **96**, 1060–1066 (2006).
37. T. J. Brodribb, S. A. M. McAdam, G. J. Jordan, S. C. V. Martins, Conifer species adapt to low-rainfall climates by following one of two divergent pathways. *Proc. Natl. Acad. Sci. U.S.A.* **111**, 14489–14493 (2014).
38. N. Martin-StPaul, S. Delzon, H. Cochard, Plant resistance to drought depends on timely stomatal closure. *Ecol. Lett.* **20**, 1437–1447 (2017).
39. Y. Sun *et al.*, Wilted cucumber plants infected by *Fusarium oxysporum* f. sp. *cucumerinum* do not suffer from water shortage. *Ann. Bot.* **120**, 427–436 (2017).
40. B. Fallon *et al.*, Spectral differentiation of oak wilt from foliar fungal disease and drought is correlated with physiological changes. *Tree Physiol.* **40**, 377–390 (2020).
41. B. Muller *et al.*, Water deficits uncouple growth from photosynthesis, increase C content, and modify the relationships between C and growth in sink organs. *J. Exp. Bot.* **62**, 1715–1729 (2011).
42. A. G. Quentin *et al.*, Non-structural carbohydrates in woody plants compared among laboratories. *Tree Physiol.* **35**, 1146–1165 (2015).
43. L. Guerin-Dubrana *et al.*, Statistical analysis of grapevine mortality associated with esca or Eutypa dieback foliar expression. *Phytopathol. Mediterr.* **52**, 276–288 (2013).
44. S. Li *et al.*, Spatial and temporal pattern analyses of esca grapevine disease in vineyards in France. *Phytopathology* **107**, 59–69 (2017).
45. G. Marchi *et al.*, Some observations on the relationship of manifest and hidden esca to rainfall. *Phytopathol. Mediterr.* **45**, S117–S126 (2006).
46. S. Serra, V. Ligios, N. Schianchi, V. A. Prota, B. Scanu, Expression of grapevine leaf stripe disease foliar symptoms in four cultivars in relation to grapevine phenology and climatic conditions. *Phytopathol. Mediterr.* **57**, 557–568 (2018).
47. C. Kraus, R. T. Voegele, M. Fischer, The esca complex in German vineyards: Does the training system influence occurrence of GLSD symptoms? *Eur. J. Plant Pathol.* **155**, 265–279 (2019).
48. M. T. Tyree, J. S. Sperry, Vulnerability of xylem to cavitation and embolism. *Annu. Rev. Plant Physiol. Plant Mol. Biol.* **40**, 19–38 (1989).
49. S. Berger, A. K. Sinha, T. Roitsch, Plant physiology meets phytopathology: Plant primary metabolism and plant-pathogen interactions. *J. Exp. Bot.* **58**, 4019–4026 (2007).
50. H. G. Jones, *Plants and Microclimate: A Quantitative Approach to Environmental Plant Physiology* (Cambridge University Press, 2013).
51. B. E. Ewers, R. Oren, Analyses of assumptions and errors in the calculation of stomatal conductance from sap flux measurements. *Tree Physiol.* **20**, 579–589 (2000).
52. B. Biais *et al.*, Remarkable reproducibility of enzyme activity profiles in tomato fruits grown under contrasting environments provides a roadmap for studies of fruit metabolism. *Plant Physiol.* **164**, 1204–1221 (2014).
53. D. I. Arnon, Copper enzymes in isolated chloroplasts. Polyphenoloxidase in *Beta Vulgaris*. *Plant Physiol.* **24**, 1–15 (1949).
54. M. Stitt, R. M. Lilley, R. Gerhardt, H. W. Heldt, Metabolite levels in specific cells and subcellular compartments of plant leaves. *Methods Enzymol.* **174**, 518–552 (1989).
55. J. H. M. Hendriks, A. Kolbe, Y. Gibon, M. Stitt, P. Geigenberger, ADP-glucose pyrophosphorylase is activated by posttranslational redox-modification in response to light and to sugars in leaves of Arabidopsis and other plant species. *Plant Physiol.* **133**, 838–849 (2003).
56. G. Bortolami *et al.*, Data for Grapevines under drought do not express esca leaf symptoms. Portail Data INRAE. https://doi.org/10.15454/SHLIHA. Deposited 8 March 2021.

www.manaraa.com